

Speckles in a highly corrected adaptive optics system

E. E. Bloemhof
Jet Propulsion Laboratory, California Institute of Technology,
Pasadena, CA USA 91109

ABSTRACT

Understanding the behavior of post-correction speckles in adaptive optics systems at very high Strehl ratio is critical to determining the ultimate effectiveness of such systems for companion searches that may eventually allow the study of extrasolar planets. Recent investigations indicate that speckles, to first order in remnant phase left by the AO system, have a strong "anomalous" component that is not included in the standard (1-S) estimates of the power in the focal plane halo. Brightness of individual anomalous speckles can exceed that of "classical" speckles by orders of magnitude, although it is expected that other unusual properties of the anomalous speckles may cause them to average away rapidly in time integrations, or be instantaneously cancelled by suitable observational techniques. For example, the anomalous speckles are also "pinned", or spatially localized, on secondary Airy maxima, causing them to be suppressed on Airy nulls; they also have zero mean over time, as well as distinct symmetry properties that might be exploited. In this paper, I explore in some detail the range of operational parameters over which anomalous speckles are problematic.

Keywords: adaptive optics, speckles, atmospheric turbulence

1. INTRODUCTION

Adaptive optics (AO) has begun to deliver remarkably good image correction at optical and near-infrared wavelengths. Using a relatively modest 16x16 array of wavefront sensing subapertures, and 241 controlled actuators on its deformable mirror, the PALAO system on the Palomar 5 meter telescope has achieved Strehl ratios $S \sim 0.60$ at K-band ($2.2 \mu\text{m}$)¹. Observations with this high degree of adaptive correction commonly reveal patterns with apparent spatial regularity and temporal persistence in the residual speckle halo, effects which have been noted by other groups^{2,3}. (In this context, persistent means enduring for many temporal update cycles $\tau_0 \sim 100$ ms for PALAO, roughly the inverse of the high-order correction bandwidth of the AO system.)

Our systematic studies of the adaptively corrected diffraction-limited point-spread function (PSF) clearly revealed persistent spatial patterns of bright intensity knots, having low-order symmetry (three- or four-fold), on the inner Airy rings at high Strehl ratio⁴. Amplitudes were not consistent with diffraction from the four-fold symmetric telescope spiders, which would in any case not explain shifts to three-fold symmetric patterns on timescales of tens of minutes. Instead, these image features are generally attributed to slowly-varying non-common-path aberrations causing the PSF calibration, which in PALAO consists of about ten low-order Zernike functions, to become outdated. In PALAO, as in most AO systems, the optical beamtrain is split into two "non-common" paths by a dichroic mirror. Visible wavelengths are directed into the wavefront sensor, a Shack-Hartmann, and infrared wavelengths into the science camera. Differing aberrations between these paths will cause errors, and the differences are calibrated only periodically; flexure will cause that calibration to become invalid, so that optical aberrations will be present in the science image although the wavefront sensor path is well corrected. Since PALAO is mounted at the telescope's Cassegrain focus, and experiences changing orientation as a celestial source is tracked, these problems are expected to be particularly important.

An example of a high-Strehl image is shown in Figure 1, obtained by PALAO with a narrow spectral filter at K-band ($2.2 \mu\text{m}$) under conditions of relatively good initial seeing. The exposure time was about 0.5 s, and an image quality of about $S = 0.6$ was achieved. The first Airy ring shows a 3-fold symmetric pattern of bright knots, but the outer part of the halo also shows speckle-like structures that appear to cluster in rings and have arc-like individual morphologies, possibly following Airy rings. (Some extremely persistent compact features in the speckle halo are ghost reflections in the PALAO optics, and the four characteristic spots near the corners of the image are of course waffle-mode artifacts.)

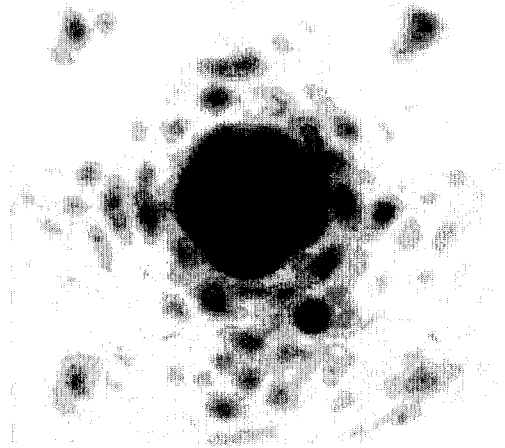
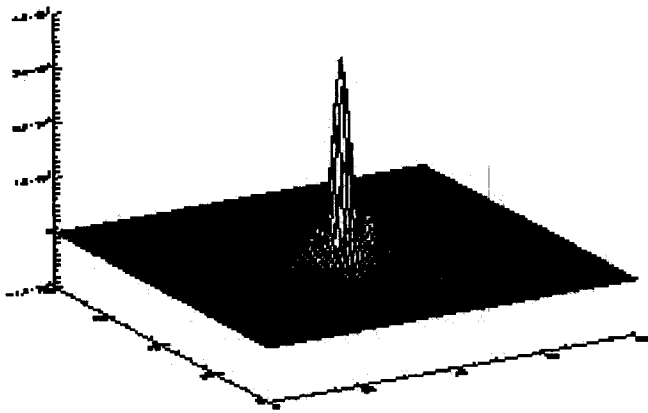


Figure 1 – Highly corrected near-infrared ($2.2 \mu\text{m}$) image from the Palomar adaptive optics system (PALAO). Initial seeing was good, allowing a final Strehl ratio in this corrected image of $S = 0.60$; exposure time was short (about 0.5 s). (Left) 3D display showing 3-fold symmetric structures on the first Airy ring, due to changing non-common-path errors. (Right) 2D intensity plot, with a logarithmic display to bring out the fainter features in the outer halo. In addition to instrumental ghosts and “waffle mode”, there are many speckles that seem to group in rings and show arc-like individual morphologies suggestive of clustering on Airy rings.

These studies suggested an interaction between the PSF and remnant aberrations in the AO system, and led to speculation as to whether the more subtle patterns that seem to exist in the outer speckle halo could also be traced to an interaction between the diffraction-limited PSF and the remnant aberrations of the turbulent atmosphere that the AO system could not correct. Since these effects were seen only at high Strehl, it was natural to seek an explanation that exploited a small-phase expansion of the complex exponential in the standard Fourier-optical expression for the image. The mathematical machinery for this is reviewed in Section 2.

Images such as the one shown in Figure 1 motivated our investigations of speckle structure in highly corrected images, and led to the deduction of the unanticipated speckle properties discussed in Sections 3 to 6. Ironically, a full empirical study of these experimental PALAO images has not yet been completed. Such a study would be extremely valuable and could solidify our understanding of the unusual effects and strategies described in the present paper, possibly uncover new effects not yet considered, and also confirm that they become relevant in the regimes of image correction (Strehl ratios $S \sim 0.6$) that are currently accessible to AO systems. But the speckle pinning, speckle symmetry, and related effects that these observations inspired are quite secure, following straightforwardly from the basic mathematics of image formation.

The discussion in this paper will be somewhat idealized in isolating the fundamental dependence of speckle behavior on remnant phase fluctuations in the pupil plane: the intensity-fluctuation component of atmospheric turbulence (“scintillation”) will be neglected. Also, an ideal telescope is assumed, and no explicit accounting is made of scattering from surface imperfections on individual mirrors in the imaging system.

2. REVIEW OF THE DERIVATION OF HIGH-STREHL SPECKLE TERMS

The derivation of speckle behavior at high adaptive correction⁵ begins with the fundamental Fourier-optical expression relating the focal-plane intensity from an unresolved guide star to the disturbance at the pupil plane, or rather to an effective pupil plane at which atmospherically induced phase perturbations have been reduced to very small “remnant” values by the corrective action of the adaptive optics system. The remnant phase function is denoted by $\phi(\xi, \eta)$ over a pupil described by the aperture function $A(\xi, \eta)$, where (ξ, η) are two spatial coordinates across the pupil, essentially the primary mirror of the telescope. Then the image-plane intensity due to remnant aberrations due to atmospheric turbulence that the AO system could not completely correct is

$$\text{Intensity}(x, y) = \left| F.T. \left[A(\xi, \eta) e^{i\phi(\xi, \eta)} \right] \right|^2 = \left| \overline{A e^{i\phi}} \right|^2 \quad (1)$$

Here the Fourier transform is denoted by F.T.[...], and also by the compact overbar notation, which is particularly useful for many algebraic manipulations. If the complex exponential in Equation (1) is expanded for small ϕ , and terms of higher than first order in ϕ are neglected, the squared modulus will result in two terms, one linear in $\hat{\Phi}$ and one quadratic:

$$\text{Intensity}(x, y) \approx \left| \overline{A} \right|^2 + 2 \text{Re} \left[i \left(\overline{A} \otimes \overline{\phi} \right) \overline{A}^* \right] + \left| \overline{A} \otimes \overline{\phi} \right|^2 \quad (2)$$

The two-dimensional convolution is here denoted by xxx, and $\text{Re}[\dots]$ denotes the real component of a complex-valued expression. The first term in Equation (2), by far the largest in amplitude, is the diffraction-limited PSF of the aperture A , while the remaining two terms are much smaller, and represent two kinds of patterns occurring in the spatially extended speckle halo. An unlimited number of additional terms may be derived in a straightforward way by keeping higher-order terms in the expansion of the complex exponential⁶, but the two speckle terms in Equation (2) will determine all the essential characteristics of the speckle halo by virtue of having much larger amplitude than any terms arising from retaining higher orders of $\hat{\Phi}$ in the expansion.

The basic physics of Equation (2) is more clearly illustrated by considering the pedagogically instructive case of a circular, unobstructed (and unapodized, or “clear”) aperture A , for which the diffraction-limited PSF, and the stellar image at perfect correction, $S = 1$, is the Airy pattern:

$$\text{PSF}(x, y) = \left| \overline{A} \right|^2 \quad (3)$$

The two speckle terms of Equation (2) then simplify to the following expression for the PSF plus speckle halo:

$$\text{Intensity}(x, y) \approx \left| \overline{A} \right|^2 - 2 \text{Im} \left[\overline{\phi} \right] \overline{A} + \left| \overline{\phi} \right|^2 \quad (4)$$

This is a useful working form that captures speckle halo behavior due to remnant phase fluctuations at high Strehl. Speckle noise has been shown by Racine et al. to be proportional to speckle intensity, and to the square root of the number of statistically independent speckle realizations that are co-added⁷. Observational evidence indicates that some effects predicted by Equation (4) may become noticeable at adaptive corrections as modest as $S = 0.6$.

A number of unusual properties of the two speckle terms in Equation (4) are immediately implied by their mathematical form, and these will be discussed in the next few sections. In Section 4, their relative magnitudes are estimated as a function of Strehl ratio and density of actuators on the deformable mirror used for image correction, which controls the number of speckles by controlling the size of the speckle halo. The magnitudes of all speckle intensities derived from retaining higher-order terms in the small-phase expansion of the exponential are much smaller, as is expected and is easily shown by application of the Rayleigh theorem of Fourier transforms⁸ term-by-term to that expansion: the lowest-order non-trivial terms, which appear in Equation (2) or Equation (4), control the essential physics of the speckle halo.

Nomenclature for the first type of high-Strehl speckle, i.e. the second term in Equation (2) or Equation (4), will sometimes be the “linear” term, for its essential linearity in $\hat{\phi}$, and sometimes the “anomalous” term, for the fact that multiplication by \hat{A} can amplify this term to anomalously high intensity not budgeted for in the usual (1-S) power budget⁷. Nomenclature for the second type of high-Strehl speckles, the third term in those equations, will sometimes be the “quadratic” term and sometimes be the “classical” term, referring to the fact that this term does account for the “classical” estimate of power in the speckle halo, (1-S).

3. SYMMETRIES OF THE HIGH-STREHL SPECKLE TERMS

The two speckle terms of Equation (2) have definite spatial symmetries, which may be useful as a practical observational tool. These symmetries are inherited from the even symmetry of \hat{A} and the Hermitian symmetry of $\hat{\phi}$, which is the Fourier transform of a real function⁸. The linear-term speckle pattern, $-2 \text{Im}(\hat{\phi})\hat{A}$, is antisymmetric with respect to spatial inversion, while the quadratic-term speckle pattern, $|\hat{\phi}|^2$, is spatially symmetric (or centrosymmetric). Centrosymmetry of speckles at high adaptive correction was noted experimentally in the context of coronagraphy by Rouan et al.⁹, and explained in terms of the small-phase expansion of the exponential by arguments similar to those just given.

Figure 1 shows numerical simulations of the two speckle terms in Equation (4) for a number of realizations of the pupil phase function $\hat{\phi}$ and resulting speckle amplitude $\hat{\phi}$. In each case, the pupil is divided into a grid of positions that may be thought of as seeing cells or as individual deformable-mirror actuators, and a random number generator is used to assign the local value of remnant phase. Intensities are not well shown, as the amplitude scales are arbitrary, but the spatial symmetry of the linear-term speckles and the antisymmetry of the quadratic-term speckles are readily apparent. Detailed examination shows that the linear speckle intensity has nulls matching those of the diffraction-limited PSF, though this is difficult to see in a casual inspection.

The distinct symmetry of the two dominant speckle terms at high adaptive correction suggests symmetry-based observational tactics to suppress one term or the other. Antisymmetrizing images (extracting the antisymmetric component) by subtracting a spatially inverted replica has been suggested for enhancing the sensitivity of high-Strehl coronagraphy⁹. This could be effective in the current case as well, if noise due to the symmetric quadratic-term classical speckles were great enough to offset the $1/\sqrt{2}$ loss of signal that would occur on deleting the symmetric component of any companion image being sought (a point-like companion would be an equal mix of symmetric and antisymmetric components). Similarly, if the antisymmetric linear-term anomalous speckles were sufficiently dominant, it could help to symmetrize an image by adding a spatially inverted replica.

It will be useful in the next section to know the spatial density of speckles in the focal plane. Being manifestations of diffraction from an aperture of diameter D , individual speckles have size of order $\sim \lambda/D$, the diffraction limit. (For PALAO at $2.2 \mu\text{m}$, this is about 0.090 arcseconds.) The spatial scale of correction applied in the pupil plane may be taken to be a , the spacing of individual actuators in the deformable mirror (often, a is roughly matched to r_0 , the transverse coherence scale of atmospheric turbulence). Then the linear size of the speckle halo is of order λ/a ; for PALAO at $2.2 \mu\text{m}$, this is about 1.6 arcseconds. The number of speckles of diameter $\sim \lambda/D$ that will fit inside a halo of diameter $\sim \lambda/a$ is of order $(D/a)^2$; Roddier¹⁰ derived the numerical prefactor to arrive at the following expression for the total number of speckles in the halo:

$$N_s \approx (0.342) \left(\frac{D}{a} \right)^2 \quad (5)$$

The simulations in Figure 2 show that the classical speckles fading out in intensity on a scale of $1/a$, as expected, and detailed examination over the full halo confirms a speckle count compatible with the prediction of Equation (5).

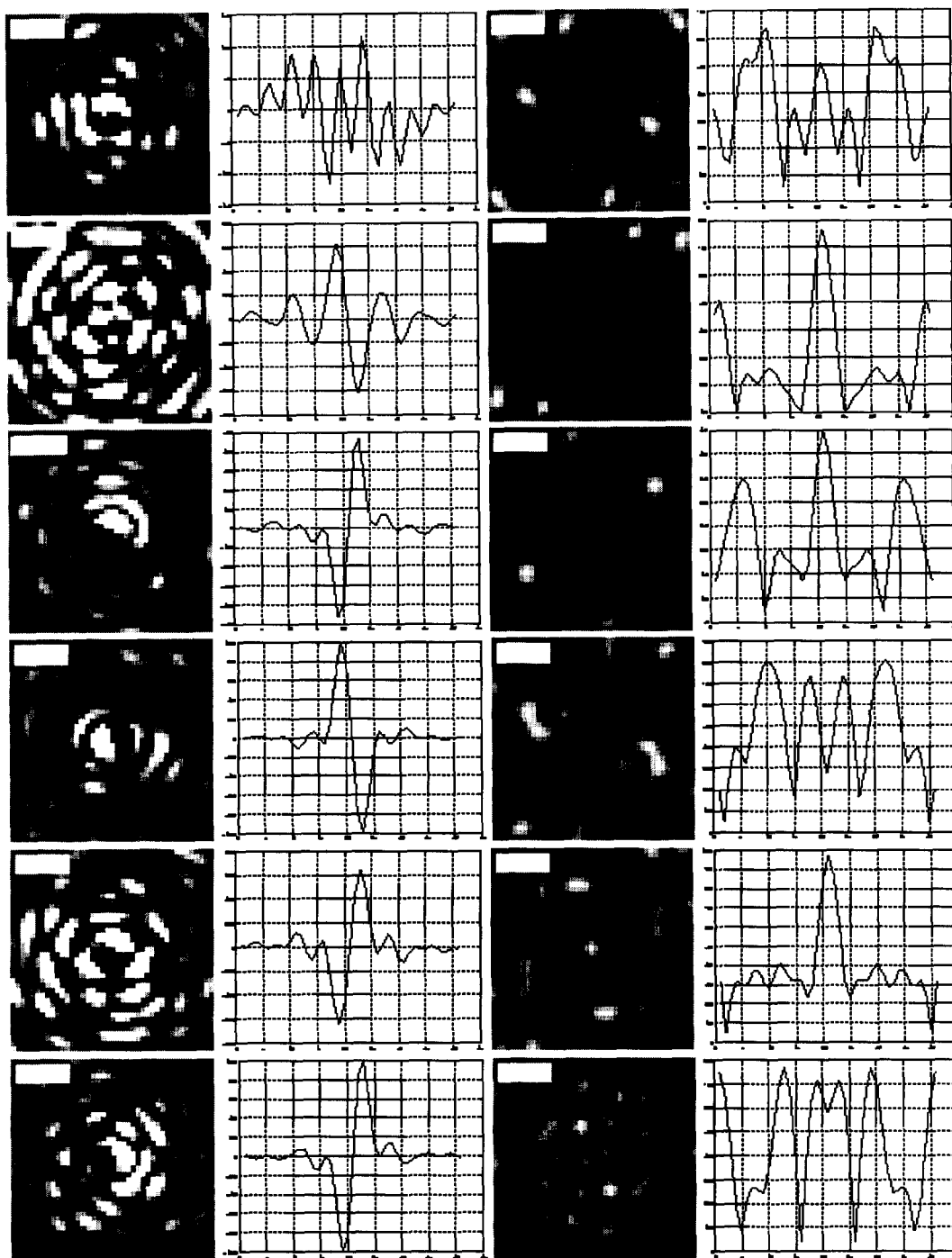


Figure 2 – Linear speckle intensity from Equation 4 (left column), a horizontal cut, the corresponding quadratic speckle intensity, and a cut through that. Each row is derived from a new, statistically independent random phase function across the pupil, $\Phi(\xi,\eta)$. Scales are arbitrary; amplitudes will depend on the Strehl ratio and density of correcting actuators. Note the antisymmetry and centrosymmetry, respectively, of the linear (anomalous) and of the quadratic (classical) speckle patterns.

4. RELATIVE INTENSITY IN “ANOMALOUS” SPECKLES vs “CLASSICAL” SPECKLES

Qualitatively, the interplay of intensity between anomalous and classical speckles can be discerned by careful study of Figure 2. For example, the third speckle realization has a speckle intensity $\hat{\phi}$ of only moderate intensity at the PSF origin, as indicated by the moderate peaks in the classical speckle pattern, $|\hat{\phi}|^2$, in the third column. By virtue of occurring where the PSF amplitude \hat{A} is large, though, this speckle amplitude produces a very bright antisymmetric signature in the anomalous speckle pattern, $-2\text{Im}\{\hat{\phi}\}\hat{A}$, in the first column.

More systematically, some simple estimates of the magnitude of anomalous speckles¹¹ may be made by estimating the magnitude of $|\hat{\Phi}|$ in Equation (4). For this purpose, the total integrated power in the speckle halo is simply the integral of the last term in Equation (4), due to the classical speckles, because the spatial integral of the antisymmetric anomalous term vanishes. The classical speckles may be thought of as a collection of N_s diffraction-limited spots of light of typical intensity we wish to calculate, where the number of speckles is given by Equation (5). The anomalous linear-term speckles, by their antisymmetry, contribute no power to the speckle halo¹², and so the total power in the halo, proportional to $(1-S)$, may be divided by N_s to give the relative power in a typical classical speckle, arising from the quadratic term, $\text{mod}\hat{\phi}^2$: (Because speckles are diffraction-limited, this power is also the measure of a typical speckle’s height, or peak intensity, as a fraction of the height of the PSF)

$$\text{quadratic intensity} \approx \frac{(S-1)}{N_s} = \frac{(S-1)}{0.342\left(\frac{D}{a}\right)^2} \quad (6)$$

With this estimate for the quadratic-term (classical) speckle intensity, $|\hat{\Phi}|^2$, it is straightforward to estimate the ratio of linear to quadratic terms (anomalous to classical, i.e. the 2nd to the 3rd term in Equation (4)):

$$\frac{|\text{linear}|}{\text{quadratic}} \approx \sqrt{2} \left| \bar{A} \right| \sqrt{\frac{S}{S-1} (0.342)\left(\frac{D}{a}\right)^2} \quad (7)$$

This Equation may be used to estimate the impact of anomalous speckles, as the speckle noise will be proportional to speckle intensity⁷.

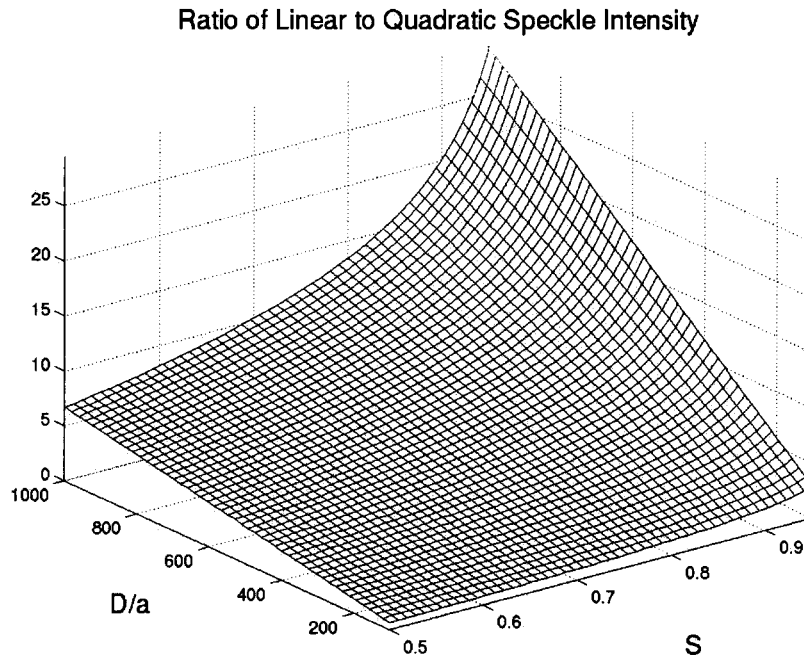


Figure 3 – Surface plot of the ratio of linear (anomalous) to quadratic (classical) speckle intensity, on the 10th Airy peak ($\hat{A}=0.00891$), as a function of Strehl ratio and DM actuator density. The ratio would be 10 times as large on the 2nd Airy peak.

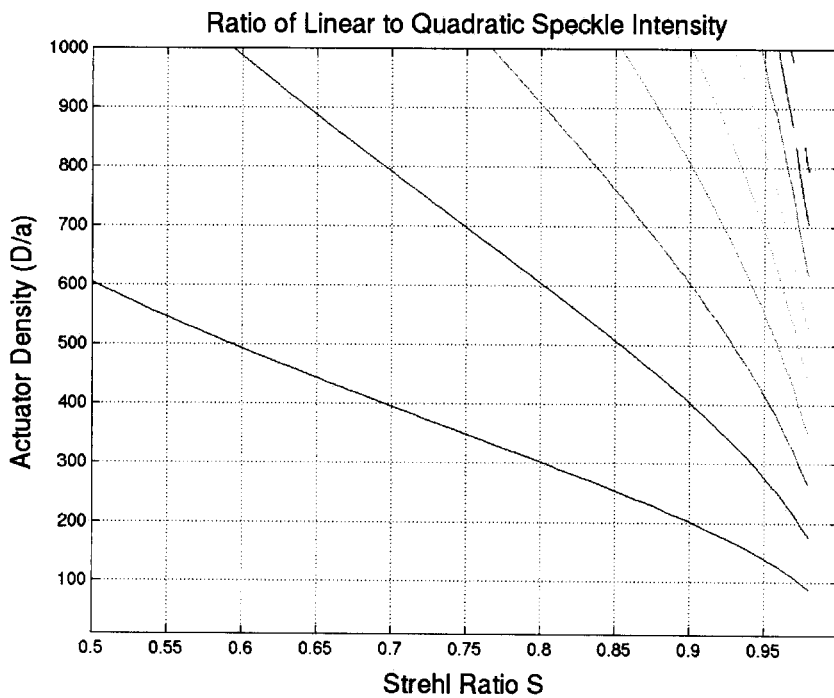


Figure 4 – Contour plot of Figure 3. Linear (“anomalous”) speckles are dominant in the upper right part of the plot; quadratic (“classical”) speckles in the lower left.

5. ZERO TEMPORAL MEAN OF ANOMALOUS SPECKLES

It was shown in Section 3 that the integral over the focal plane of any instantaneous realization of the anomalous, linear-term speckle pattern vanishes, as a result of that pattern's spatial antisymmetry. A related consequence is that anomalous speckles are as likely to have negative intensity (surface brightness) as positive (they can only occur on non-zero Airy rings, and carve into their intensity, so the net surface brightness is always non-negative). Hence, statistically-independent speckle realizations will tend to cancel out, and a long time integration at a given point in the speckle halo will sum to zero: the anomalous speckle noise term has zero temporal mean at any point in the halo.

A simple tactic for avoiding excess speckle noise from anomalous speckles is then to integrate over many correction cycles, τ_0 , of the AO system; this will result in a speckle noise level consistent with the classical prediction, $(1-S)$. Rather than assuming that each new cycle produces a statistically independent realization of the remnant speckle pattern, some more realistic assumptions about the AO system and its control loop must be made to determine how long this time is, and how reliably the anomalous speckle noise term integrates to zero. There have been indications that coherence times in actual AO systems will be longer than current idealized assumptions¹³, so this area seems worth further investigation.

6. "PINNING" AND "REGULATION" OF ANOMALOUS SPECKLES

The natural time averaging of zero-mean anomalous speckles described in the previous section makes some assumptions about the temporal behavior of the AO system: it is assumed to produce a residual phase function $\phi(\xi, \eta)$ that is spatially uncorrelated and also statistically independent of earlier residuals, on a short timescale comparable to τ_0 . It has been proposed that real AO systems may have much longer correlation timescales^{xx}, in which case the anomalously large amplitude speckles will not vanish as quickly with simple long time integrations.

There are some special cases in which excess speckle noise due to anomalous linear-term speckles can be defeated by observational techniques. These make use of the fact that the linear-term speckles have the PSF (Airy pattern) imposed upon them by the multiplicative appearance of the PSF amplitude, A -hat, in Equations 2 and 4. It follows that the linear-term speckles vanish on nulls of the Airy pattern. This fact is termed "pinning" of the speckles to Airy maxima.

One might consider observing on the Airy nulls to take advantage of this reduction of speckle noise, even in short exposures. Schematically, such an observation is drawn in Figure xx, where one pixel of the science camera CCD is carefully positioned on the 10th Airy null. Since remnant speckles are diffraction-limited, they will have spatial scales no smaller than λ/D , and so ϕ -hat will be relatively constant over a pixel small compared to this. Then the linear-term anomalous speckles will have a radial dependence that is approximately linear, inherited from the linear zero-crossing of the PSF amplitude, A -hat, so the total linear-term speckle intensity integrated over that pixel vanishes.

“Regulated” Speckle Intensity on Airy Null:

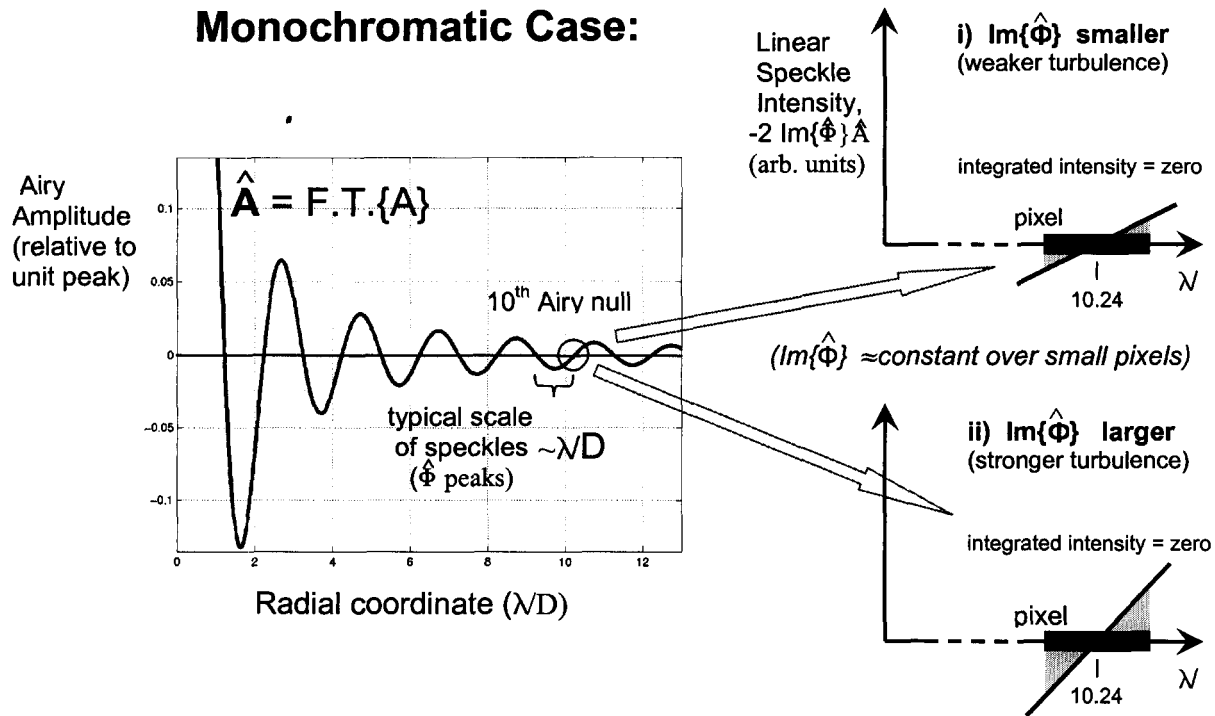


Figure 5 – Schematic illustration of “regulated” vanishing linear-term speckle intensity across a small pixel located on an Airy null, for the simplest case (monochromatic illumination). The speckle amplitude $\hat{\Phi}$ is roughly constant over a pixel small compared to λ/D , so the linear speckle intensity term inherits sign changes at the zeroes of \hat{A} . The total intensity integrated over the pixel is regulated to zero if the pixel is symmetrically positioned on the null of \hat{A} , as the shaded integrals cancel regardless of the turbulent strength.

As indicated in Figure 2, the vanishing integral of anomalous linear-term speckle noise across a pixel carefully positioned on an Airy null is regulated to be zero regardless of the strength of the turbulence or the precise quality of the adaptive correction, as long as it is high: the strength of the remnant $\text{Im}\{\hat{\Phi}\}$ simply controls the slope of the linear intensity term as it crosses the Airy null. Also from Figure 2, it is apparent that regulation to a non-zero value is not possible.

The situation in Figure 2 was diagrammed assuming monochromatic observations, for simplicity, but regulation at an Airy null will still occur for polychromatic light. If the bandwidth is relatively narrow, the single wavelength in Figure 2 is replaced by a bundle of straight lines crossing zero at slightly different x-intercepts, and the radial axis must be labeled in arcseconds rather than in units of λ/D . The net speckle intensity registered by a pixel is now the result of an integral over wavelength, as well as the spatial integral previously assumed, and there will be a pixel position at which this integral vanishes; this will be regulated as well.

Finally, more detailed investigation reveals cancellation of linear-term anomalous speckle noise will occur for relatively broad spectral bandwidths and pixel sizes, if they are appropriately positioned. Since all the components that sum to give the net intensity are proportional to a common factor of $\text{mod}\{\hat{\Phi}\}$, a vanishing sum will be regulated. This

regulated cancellation marks the first observational quantity in AO that is robust with respect to fluctuations in the seeing strength or quality of the adaptive correction.

7. CONCLUSIONS AND FUTURE DIRECTIONS

The picture that emerges is that the classical estimates of power in the speckle halo, $(1-S)$, traditionally used in estimating how well future AO systems will have to perform to reduce speckle intensity below some threshold for planet detection¹³, describes only the classical, quadratic-term speckles (the third term in Equations 2 or 4). They provide an estimate that is relevant still, if the anomalous speckles, which may be of much greater local intensity, are first reduced by the techniques of Sections 5 and 6: long time integrations, observations on Airy nulls, averages over wavelength. Those speckles are always present at this strength, and they are free to move anywhere within the speckle halo of diameter $1/a$, though they have a centrosymmetry that might be exploited to reduce their effects.

The impact of the bright, anomalous speckles on highly-corrected adaptive imaging depends on the degree to which their spatial and temporal properties can be used to cancel them out. In short exposures, representing a single random realization of the speckle pattern, anomalous speckles at $S=0.99$ will have roughly ten times the intensity of classical speckles on the tenth Airy ring, and ~ 100 times the intensity on the second Airy ring. A detector appropriately located on an Airy null, even for broad spectral bandwidth, can exploit the spatial antisymmetry of the anomalous speckle pattern to obtain a high degree of cancellation even in short exposures. In long exposures, the antisymmetry of the anomalous pattern gives it a vanishing temporal mean everywhere in the image, so speckle noise will approach the limits set by $(1-S)$, an estimate of speckle power that includes only the classical speckles. (The instantaneous integral of intensity of the anomalous speckles over an image vanishes, as the pattern is antisymmetric, so they contribute no power.)

In principle the temporal cancellation of anomalous speckles will be rapid, as they may change sign from one realization to the next. But it is important to determine how reliably the cancellation proceeds in practice, particularly since temporal or spatial correlations, or long-term instrumental biases, may mean that a real AO system does not deliver a statistically independent speckle realization with each cycle time τ_0 . It has been suggested⁶ that this assumption, though a logical limiting case and useful in analyzing the most fundamental limitations of companion searches with adaptive optics¹³, may not strictly hold in practice, and actual coherence times of AO systems may be substantially longer. This would have the effect of making the higher speckle noise due to anomalous speckles more long-lasting, and the effects and techniques discussed in the present paper all the more important.

The remnant phase effects isolated and discussed here are a large component of the problem of imaging with high adaptive correction, and as such will play an important role in the design and use of instruments being planned to search for exosolar planets¹³.

ACKNOWLEDGMENTS

The research described in this publication was carried out at the Jet Propulsion Laboratory, California Institute of Technology, under a contract with the National Aeronautics and Space Administration.

8. REFERENCES

1. M. Troy, R. G. Dekany, B. R. Oppenheimer, E. E. Bloemhof, T. Trinh, F. Dekens, F. Shi, T. L. Hayward, and B. Brandl, "Palomar Adaptive Optics Project: Status and Performance", *Proc. SPIE*, Vol. **4007**, pp. 31-40, 2000
2. U. Arizona, private communication. (spatial regularities, persistent speckles in halo)
3. U. Hawaii, private communication ("")
4. E. E. Bloemhof, K. A. Marsh, R. G. Dekany, M. Troy, J. Marshall, B. R. Oppenheimer, T. L. Hayward, and B. Brandl, "Stability of the Adaptive-Optic Point-spread Function: Metrics, Deconvolution, and Initial Palomar Results", *SPIE*, Vol. **4007**, pp. 889-898, 2000
5. E. E. Bloemhof, R. G. Dekany, M. Troy, and B. R. Oppenheimer, "Behavior of Remnant Speckles in an Adaptively Corrected Imaging System", *Ap.J.*, **558**, pp. L71-L74, 2001
6. A. Sivaramakrishnan, "Speckle Decorrelation and Dynamic Range in Speckle Noise-Limited Imaging", *Ap.J.*, **581**, pp. L59-L62, 2002
7. R. Racine, G. A. H. Walker, D. Nadeau, R. Doyon, and C. Marois, "Speckle Noise and the Detection of Faint Companions", *Pub. Astron. Soc. Pac.*, **111**, pp. 587-594, 1999
8. R. N. Bracewell, "The Fourier Transform and its Applications (2nd edition)", McGraw-Hill, New York, NY
9. D. Rouan, P. Riaud, A. Boccaletti, Y. Clénet, and A. Labeyrie, "Title", *Pub. Astron. Soc. Pac.*, **112**, pp. 1479-xxxx, 2000
10. F. Roddier, "The Effects of Atmospheric Turbulence in Optical Astronomy", *Prog. Opt.*, **19**, pp. 281-376, 1981
11. E. E. Bloemhof, "Suppression of Speckle Noise by Speckle Pinning in Adaptive Optics", *Ap.J.*, **582**, pp. L59-L62, 2003
12. E. E. Bloemhof, *Opt Lett.*, submitted.
13. J. R. P. Angel, "Ground-based imaging of extrasolar planets using adaptive optics", *Nature*, **368**, pp. 203-207, 1994